# Crucial role of quantum entanglement in bulk properties of solids

Časlav Brukner,[1,2,3] Vlatko Vedral,[4,5] and Anton Zeilinger[1,2]
[1]*Institut für Experimentalphysik, Universität Wien, Boltzmanngasse 5, A-1090 Wien, Austria*
[2]*Institut für Quantenoptik und Quanteninformation, Österreichische Akademie der Wissenschaften, Boltzmanngasse 3, A-1090 Wien, Austria*
[3]*The Blackett Laboratory, Imperial College, Prince Consort Road, London, SW7 2BW, United Kingdom*
[4]*The School of Physics and Astronomy, University of Leeds, Leeds LS2 9JT, United Kingdom*
[5]*The Erwin Schrödinger Institute for Mathematical Physics, Boltzmanngasse 9, A-1090 Vienna, Austria*
(Received 3 October 2005; published 23 January 2006)

We demonstrate that two well-established experimental techniques of condensed-matter physics, neutron-diffraction scattering and measurement of magnetic susceptibility, can be used to detect and quantify macroscopic entanglement in solids. Specifically, magnetic susceptibility of copper nitrate (CN) measured in 1963 cannot be described without presence of entanglement. A detailed analysis of the spin correlations in CN as obtained from neutron-scattering experiment from 2000 provides microscopic support for this interpretation and gives the value for the amount of entanglement. We present a quantitative analysis resulting in the critical temperature of 5 K in both, completely independent, experiments below which entanglement exists.

DOI: 10.1103/PhysRevA.73.012110 PACS number(s): 03.65.Ud, 03.67.−a

Entangled quantum systems can exhibit correlations that cannot be explained on the basis of classical laws. Since the birth of quantum theory, such correlations have been used to highlight a number of counter-intuitive phenomena, such as the Einstein-Podolsky-Rosen paradox [1] or quantum nonlocality [2]—the conflict between quantum mechanics and local realism as quantified by violation of Bell's inequalities. In recent years entanglement was realized to be a crucial resource that allows for powerful communication and computational tasks that are not possible classically [3].

The existence of quantum entanglement is generally not seen beyond the atomic scale. Only very recently entanglement experiments were realized with increasingly complex objects, either by entangling more and more systems with each other [4], or by entangling systems with a larger number of degrees of freedom [5]. Moving towards demonstration of entanglement at even larger scales will tackle the question on limits on mass, size, and complexity of systems that still can contain entanglement. The usual arguments against seeing entanglement on macroscopic scales is that large objects contain a large number of degrees of freedom that can interact with environment, inducing decoherence that ultimately leads to a quantum-to-classical transition.

Remarkably, macroscopic entanglement in solids, that is, entanglement in the thermodynamical limit of an infinitely large number of constituents of solids, was theoretically predicted to exist even at moderately high temperatures [6–10]. Recently, it was demonstrated that entanglement can even affect macroscopic thermodynamical properties of solids [8,11–15], such as its magnetic susceptibility or heat capacity, albeit at very low temperature (few mK) and only for a special material system—the insulating magnetic salt $LiHo_xY_{1-x}F_4$ [15]. This extraordinary result shows that entanglement can have significant macroscopic effects.

Nevertheless, it is an open question which macroscopic quantities can be used as entanglement witnesses for broader classes of solid-state systems. Entanglement witnesses are observables which, by our convention, have positive expectation values for separable states and negative ones for some entangled states [16]. Finally, an exact experimental quantification of entanglement, in the form of inferring a measure of entanglement between microscopic constituents of solids, has been an experimental challenge. Note that the nonzero value of the spin-spin correlation function does not necessarily imply the existence of entanglement. This is why it is difficult to separate quantum and classical correlations, and we need to combine both standard techniques of solid state as well as the machinery of quantum information theory in order to witness macroscopic entanglement. What we need, for detection of spin entanglement, for example, are sufficiently strong spin-correlations in all three orthogonal spatial directions, and they need to be combined in a specific way to reveal entanglement.

Here we demonstrate that experimental techniques of condensed-matter physics can be used to detect and quantify entanglement in solids. We will use already published experimental results of both microscopic structure and macroscopic properties of the spin-1/2 alternating bond antiferromagnet CN $[Cu(NO_3)_2 2.5D_2O]$. In the first approach we analyze experimental results of neutron scattering on CN performed in 2000 [17] and show that they provide experimental quantification of macroscopic entanglement in solids. The experimentally obtained dynamic spin correlations for next neighboring sites enables us to determine concurrence [18]—a measure of bipartite entanglement—and show the existence of entanglement at moderately high temperatures (as high as 5 K). In the second, parallel, approach we show that magnetic susceptibility at zero magnetic field is a macroscopic thermodynamical entanglement witness for the class of solid-state systems that can be modeled by a strongly alternating spin-1/2 antiferromagnet chain. We then show that the measured values for magnetic susceptibility of CN in 1963 [19] imply the presence of entanglement in the same temperature range (below 5 K).

CN is an accurate realization of a strongly alternating one-dimensional antiferromagnetic Heisenberg spin chain.

 

The corresponding spin Hamiltonian is given by

$$H = \sum_j (J_1 \mathbf{S}_{2j} \cdot \mathbf{S}_{2j+1} + J_2 \mathbf{S}_{2j+1} \cdot \mathbf{S}_{2j+2}), \quad (1)$$

representing pairs of spins that are alternately coupled by strong intradimer $J_1 \approx 0.44$ meV and weak interdimer $J_2 \approx 0.11$ meV coupling [20]. This can be described by a model of antiferromagnetically coupled spin pairs—dimers—which are themselves coupled by weaker antiferromagnetic interaction. The model has a highly entangled nontrivial spin-0 ground state [21,22] and for all $0 \leqslant J_2/J_1 < 1$ has a gap of the order of $\Delta \approx J_1$ to the first excitation, which is a band of spin-1 excitations (magnons). However, because here $J_2/J_1 \approx 0.24$ [17,20], it is useful to think of CN as a chain of uncoupled spin dimers. Each dimer then has a singlet ground state and the triplets are the degenerate excited states. The existence of the energy gap gives an estimate for persistence of entanglement for temperature range below $T \approx J_1/k \approx 5K$, where $k$ is the Boltzmann constant.

Next we describe the main experimental results of Ref. [17]. We will follow the discussion given there. CN has a monoclinic crystal structure with space group $I12/c1$ and with low-temperature parameters $a=16.1$ Å, $b=4.9$ Å, $c=15.8$ Å, and $\beta=92.9°$. The vector connecting dimers center to center is $\mathbf{u}_0=[111]/2$ for half the chain, and $\mathbf{u}'_0=[1\bar{1}1]/2$ for the other half. The corresponding intradimer vectors are $\mathbf{d}_1=[0.252, \pm 0.027, 0.228]$, respectively. In the experiment the neutron-scattering intensity was measured in the temperature range $0.31 < T < 7.66$ K (i.e., $0.06J_1 < kT < 1.5J_1$) as a function of energy transfer $\hbar\omega$ and wave-vector transfer $\mathbf{Q}$. Count rates were normalized to incoherent elastic scattering from the sample to provide absolute intensity $\tilde{I}(\mathbf{Q},\omega)=|(g/2)F(Q)|^2 2S(\mathbf{Q},\omega)$. Here $g=\sqrt{(g_b^2+g_\perp^2)/2}=2.22$ with $g_b=2.31$ and $g_\perp=2.11$ that show small anisotropy of $g$ factor along and perpendicular to the crystallographic direction $\mathbf{b}$ [20], $F(Q)$ is the magnetic form factor for $Cu^{2+}$ [23], and $S(\mathbf{Q},\omega)$ is the scattering function [24].

The direct link between the microscopic structure as given by the correlation function between spins and the intensity of inelastic neutron scattering is given by an exact sum rule (the first $\omega$ moment of scattering cross section) [25]

$$\hbar\langle\omega\rangle_{\mathbf{Q}} \equiv \hbar^2 \int_{-\infty}^{+\infty} S(\mathbf{Q},\omega) d\omega$$

$$= -\frac{1}{3} \sum_{\mathbf{d}} J_{\mathbf{d}} \langle \mathbf{S}_0 \cdot \mathbf{S}_{\mathbf{d}} \rangle (1 - \cos \mathbf{Q} \cdot \mathbf{d}), \quad (2)$$

where $\{\mathbf{d}\}$ is the set of all bond vectors connecting a spin to its neighbors, $S(\mathbf{Q},\omega)$ is the single site normalized, and $\langle \mathbf{S}_0 \cdot \mathbf{S}_{\mathbf{d}} \rangle \equiv \langle S_0^x S_{\mathbf{d}}^x \rangle + \langle S_0^y S_{\mathbf{d}}^y \rangle + \langle S_0^z S_{\mathbf{d}}^z \rangle$ is the sum over correlations for three orthogonal directions $x$, $y$, and $z$.

The intradimer correlation $\langle \mathbf{S}_0 \cdot \mathbf{S}_{\mathbf{d}_1} \rangle$ between next-neighboring spins was extracted from the global fits of the following phenomenological form for $S(\mathbf{Q},\omega)$ to the complete data set at each of temperatures (more than 1000 data points per parameter were used):

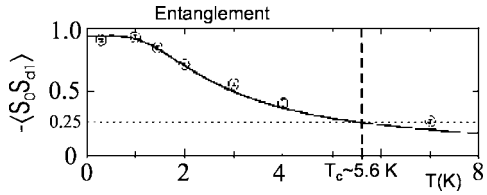


FIG. 1. The temperature dependence of spin correlation function $\langle \mathbf{S}_0 \cdot \mathbf{S}_{\mathbf{d}_1} \rangle$ for neighboring sites in CN. The figure is taken from Ref. [17]. The open circles correspond to the temperatures at which measurements were performed, the solid line was obtained from fits in Ref. [17]. The dashed line is from this work. It distinguishes temperature ranges with and without entanglement in CN. The critical temperature is around $T_c^{exp} \approx 5$ K and 0.25 on the $y$ axis is the maximal value for $\langle \mathbf{S}_0 \cdot \mathbf{S}_{\mathbf{d}_1} \rangle$ achievable with separable states. For $T < T_c^{exp}$ concurrence is given by $C = -2\langle \mathbf{S}_0 \cdot \mathbf{S}_{\mathbf{d}_1} \rangle - (1/2)$ and has the same functional dependence on temperature as given in the figure. For $T \geqslant T_c^{exp}$, $C$ vanishes.

$$S(\mathbf{Q},\omega) = \frac{\hbar\langle\omega\rangle_{\mathbf{Q}}}{\epsilon(\mathbf{Q})} \frac{1}{1 - \exp[-\beta\epsilon(\mathbf{Q})]} f[\hbar\omega - \epsilon(\mathbf{Q})]. \quad (3)$$

Here $\beta = 1/(kT)$, $\hbar\langle\omega\rangle_{\mathbf{Q}}$ stands for expression (2), $f(E)$ is a normalized spectral function, and $\epsilon(\mathbf{Q})$ is the dispersion relation. Equation (3) represents the "single mode approximation" which is valid for sufficiently low temperatures [25,26]. The dispersion relation is used in the variational form based on the first-order perturbation theory [27],

$$\epsilon(\mathbf{Q}) = J_1 - \frac{1}{2} \sum_{\mathbf{u}} J_{\mathbf{u}} \cos \mathbf{Q} \cdot \mathbf{u}, \quad (4)$$

where $J_{\mathbf{u}}$ are the same constants as $J_{\mathbf{d}}$ but the vectors $\{\mathbf{u}\}$ now connect neighboring dimers center to center both within and between the chains.

At $T=0.3$ K, $f(E)=\delta(E)$ was used and the global fit was obtained with an overall factor and four exchange coupling constants ($J_1$, $J_2$ and the constants $J_L$, $J_R$ for coupling between the chains [17]) in Eq. (4) as the only fit parameters. The fit gives $\langle \mathbf{S}_0 \cdot \mathbf{S}_{\mathbf{d}_1} \rangle = -0.9(2)$ and is within the error in agreement with the minimal possible value of $-3/4$ for dimers in the singlet state. To perform the fit at higher temperatures the spectral function was replaced by a normalized Gaussian with half width at half maximum $\Gamma(\tilde{q}) = \Gamma_0 + (\Gamma_1/2)\cos\tilde{q}$, where $\tilde{q} = \mathbf{Q} \cdot \mathbf{u}_0$ is the wave-vector transfer along the chain. Also, the dispersion relation (4) was replaced by the form $\epsilon(\mathbf{Q}) = J_1 - n(T)(1/2)\Sigma_{\mathbf{u}} J_{\mathbf{u}} \cos \mathbf{Q} \cdot \mathbf{u}$, where the renormalization factor $n(T)$ was introduced to account for finite temperatures. The prefactor for global fits at each temperature yields the intradimer spin correlations $\langle \mathbf{S}_0 \cdot \mathbf{S}_{\mathbf{d}_1} \rangle$ as given in Fig. 1. The correlations decrease with temperature increase due to mixing of the triplets with the singlet state.

We will now show that the values estimated for the correlation function can only be explained if entanglement is present in the solid. We first show that $|\langle \mathbf{S}_0 \cdot \mathbf{S}_{\mathbf{d}_1} \rangle|$ is an entanglement witness. The proof is based on the fact that for any product state of a pair of the spins one has

$$|\langle \mathbf{S}_0 \cdot \mathbf{S}_{\mathbf{d}_1} \rangle| = |\langle S_0^x \rangle \langle S_{\mathbf{d}_1}^x \rangle + \langle S_0^y \rangle \langle S_{\mathbf{d}_1}^y \rangle + \langle S_0^z \rangle \langle S_{\mathbf{d}_1}^z \rangle| \leq |\mathbf{S}_0||\mathbf{S}_{\mathbf{d}_1}| \leq 1/4. \quad (5)$$

This bound, known in solid-state physics as quantum-classical boundary, is thus an entangle-separable boundary. Here and throughout the paper we choose units to be consistent with those of Ref. [17]; spin is expressed in units of 1/2; $\hbar=1$. The upper bound was found by using the Cauchy-Schwarz inequality and knowing that for any state $|\mathbf{S}| \equiv \sqrt{\langle S^x \rangle^2 + \langle S^y \rangle^2 + \langle S^z \rangle^2} \leq 1/2$. The proof is also valid for any convex sum of product states of two spins (separable states): $\rho = \Sigma_k w_k \rho_k^1 \otimes \rho_k^2$ with $\Sigma_k w_k = 1$. In Fig. 1 the value of 1/4 for $-\langle \mathbf{S}_0 \cdot \mathbf{S}_{\mathbf{d}_1} \rangle$ distinguishes temperatures ranges with and without entanglement in CN. The critical temperature is found to be $T_c^{exp} \approx 5$ K. The reported error in the correlation function ($\Delta=0.2$ at $T=0.3$ K [17]) implies an error of around $\Delta T \approx 1$ K in the critical temperature.

Within the model of uncoupled dimers the isotropy of Heisenberg interaction in spin space ensures that $\langle S_0^x S_{\mathbf{d}_1}^x \rangle = \langle S_0^y S_{\mathbf{d}_1}^y \rangle = \langle S_0^z S_{\mathbf{d}_1}^z \rangle$ and concurrence is given by $C = 2\max[0, -\langle \mathbf{S}_0 \cdot \mathbf{S}_{\mathbf{d}_1} \rangle - (1/4)]$. Similarly, Bell's parameter—the quantum value of Bell's expression in the Clauser-Horne-Shymony-Holt inequality [28]—is given by $(8\sqrt{2}/3)|\langle \mathbf{S}_0 \cdot \mathbf{S}_{\mathbf{d}_1} \rangle|$. It is higher than the local realistic limit 2 at temperatures below $T_c^{exp}$. Apart from rescaling, both the temperature dependency of concurrence and of Bell's parameter have the same functional form as the correlation function in Fig. 1.

The temperature dependence of $\langle \mathbf{S}_0 \cdot \mathbf{S}_{\mathbf{d}_1} \rangle$ in Fig. 1 is within the error in a good agreement with a model of uncoupled dimers for which $\langle \mathbf{S}_0 \cdot \mathbf{S}_{\mathbf{d}_1} \rangle = -(3/4)\Delta n(\beta J_1)$, where $\Delta n(\beta J_1) = (1 - e^{-\beta J_1})/(1 + 3e^{-\beta J_1})$ is the singlet-triplet population difference [17]. Within the model the theoretical temperature dependence of concurrence is given by $C = \max[0, (1 - 3e^{-\beta J_1})/(1 + 3e^{-\beta J_1})]$, as obtained in Refs. [6,7]. The theoretical value for the critical temperature $T_c^{th} = J_1/(k \ln 3) = 4.6$ K is in excellent agreement with the value estimated from the experiment.

We now proceed with our second approach. We will analyze experimental results of a magnetic susceptibility measurement of CN [19] to show that the values at low temperatures cannot be explained without entanglement. This will be based on a general proof that magnetic susceptibility of any strongly alternating antiferromagnetic spin-1/2 chain is an entanglement witness.

When the system is in thermal equilibrium under a certain temperature $T$, its state is $\rho = e^{-H/kT}/Z$, where $Z = \mathrm{Tr}(e^{-H/kT})$ is the partition function and $H$ is the Hamiltonian. If $[H, M_\alpha] = 0$, the magnetic susceptibility along direction $\alpha$ is given as $\chi_\alpha \equiv (\partial \langle M_\alpha \rangle / \partial B) = (g^2 \mu_B^2 / kT)[\langle (M_\alpha)^2 \rangle - \langle M_\alpha \rangle^2]$, where $\langle M_\alpha \rangle$ is magnetization along $\alpha$, $M_\alpha = \Sigma_j S_j^\alpha$, $B$ is external magnetic field, $g$ is $g$ factor, and $\mu_B$ is the Bohr magneton. Because of the isotropy of the Hamiltonian in spin space, $\langle M_\alpha \rangle$ at zero field vanishes for any temperature. This implies the following form for magnetic susceptibility at zero field: $\chi_\alpha = (g^2 \mu_B^2 / kT) \langle (M_\alpha)^2 \rangle_{B=0} = (g^2 \mu_B^2 / kT) \Sigma_{i,j} \langle S_i^\alpha S_j^\alpha \rangle \approx (g^2 \mu_B^2 N / kT)[(1/4) + \langle S_0^\alpha S_{\mathbf{d}_1}^\alpha \rangle]$. Here

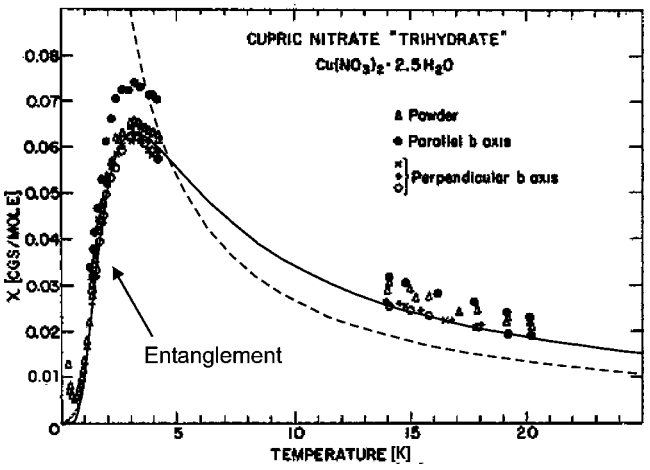


FIG. 2. The temperature dependence of magnetic susceptibility of powder CN (triangles) and a single-crystal CN measured at low-field parallel (open squares) and perpendicular (open circles, crosses, filled circles) to the monoclinic $b$ axis. The data and the figure are from Ref. [19]. The solid curve is the theoretical curve for a dimer rescaled for the amount of noise estimated from the experiment. This noise is computed as the ratio of the maximal experimental value (averaged over crystal data) and the maximal theoretical value. The dashed curve represents the macroscopic entanglement witness (6) and is rescaled in exactly the same way. The intersection point of this curve and the experimental one defines the temperature range (left from the intersection point) with entanglement in CN. The critical temperature is around $T_c^{exp} \approx 5$ K. Note that the entanglement witness will cut the experimental curve (and hence yield a critical temperature) independently of a particular rescaling procedure.

we assume that correlations between all spins that are not nearest neighbors are negligible compared with $\langle S_0^\alpha S_{\mathbf{d}_1}^\alpha \rangle$. This approximation is valid for our case of strongly alternating spin chains at low temperatures. It is important to note that apart from the weak anisotropy in the $g$ factor, the magnetic susceptibility at zero field is isotropic, i.e., $\chi_x = \chi_y = \chi_z \equiv \chi$. Thus if we sum the values of magnetic susceptibilities over the three orthogonal directions $x$, $y$, and $z$ in space we obtain $\chi = (g^2 \mu_B^2 N / kT)[(1/4) + (\langle \mathbf{S}_0 \cdot \mathbf{S}_{\mathbf{d}_1} \rangle / 3)]$, where the mean value $\langle \cdots \rangle$ is taken over the thermal state at $B=0$. However, because one has $|\langle \mathbf{S}_0 \cdot \mathbf{S}_{\mathbf{d}_1} \rangle| \leq 1/4$ for any separable state [Eq. (5)], the magnetic susceptibility for such states is limited as given by

$$\chi \geq \frac{g^2 \mu_B^2 N}{kT} \frac{1}{6}. \quad (6)$$

Thus a violation of this inequality necessarily detects entanglement in the system. Interestingly, concurrence for such system can be expressed solely in terms of magnetic susceptibility: $C = \max[0, (6kT\chi)/(Ng^2\mu^2) + 1]$.

In Ref. [19] magnetic susceptibility of CN was measured on single crystal in 0.4–4.2- and 14–20-K ranges of temperature. The measurement method was based on a mutual inductance bridge working at 275 Hz. The susceptibility was found to have a rounded maximum at 3.2 K dropping very

rapidly below this temperature approaching zero at vanishing temperatures, as given in Fig. 2. Such behavior is typical for alternating spin chains. Thermodynamical entanglement witness (6) is represented by the dashed line in Fig. 2. The measured values of magnetic susceptibility below the intersection point of the curve representing the witness and the experimental curve cannot be described without entanglement. The critical temperature is around $T_c^{exp} \approx 5$ K. This is in excellent agreement with the value estimated from the neutron-scattering experiment in spite of the fact that different samples were used (the authors of Ref. [19] noted possible variations of the physical state of the sample due to high hygroscopy of CN), the two experimental methods test entirely different physical quantities and are almost 40 years apart (no experimental error of magnetic susceptibility measurement was reported in Ref. [19]).

In conclusion, we show that neutron-scattering experiments [17] and measurement of magnetic susceptibility [19] demonstrate the presence of macroscopic quantum entanglement in a solid (cupric nitrate) and enable its quantification. We believe our results indicate that entanglement may play a broad generic role in macroscopic phenomena.

The question of having macroscopic entanglement is fascinating in its own right. Its demonstration pushes the realm of quantum physics well into the macroscopic world, thus opening the possibility to test quantum theory versus alternative theories well beyond the scales on which theirs predictions coincide. It also has important practical implications for implementation of quantum information processing. If the future quantum computer is supposed to reach the stage of wide commercial application, it is likely that it should share the same feature as the current (classical) information technology and be based on solid-state systems. It will thus be important to derive the critical values of physical parameters (e.g., the high-temperature limit) above which one cannot harness quantum entanglement in solids as a resource for quantum information processing.

We consider our work to imply that many experiments performed in the past may still hide different and interesting physics. Experiments of Berger *et al.* [19] from 1963 and Xu *et al.* [17] from 2000 used here are exemplary. Interestingly, the 1963 experiment was performed long before any serious attempts to measure entanglement began in the 1970s. It is not even impossible that we are able to find a result from which we can infer the existence of entanglement and which appeared well before this concept was conceived by Schrödinger in 1935.

This work has been supported by the Austrian Science Foundation (FWF) Project SFB 1506 and European Commission (RAMBOQ). Č.B. and V.V. thank the British Council in Austria.

[1] A. Einstein, B. Podolsky, and N. Rosen, Phys. Rev. **47**, 777 (1935).
[2] J. S. Bell, Physics (Long Island City, N.Y.) **1**, 195 (1964).
[3] M. A. Nielsen and I. L. Chuang, *Quantum Computation and Quantum Information* (Cambridge University Press, Cambridge, England, 2000).
[4] J.-W. Pan *et al.*, Nature (London) **403**, 515 (2000); Z. Zhao *et al.*, *ibid.* **430**, 54 (2004); B. Julsgaard, A. Kozhekin, and E. S. Polzik, *ibid.* **413**, 400 (2001).
[5] A. Mair *et al.*, Nature (London) **412**, 313 (2001).
[6] M. A. Nielsen, Ph.D. thesis, University of New Mexico, 1998, e-print quant-ph/0011036.
[7] M. C. Arnesen, S. Bose, and V. Vedral, Phys. Rev. Lett. **87**, 017901 (2001).
[8] K. M. O'Connor and W. K. Wootters, Phys. Rev. A **63**, 052302 (2001).
[9] T. J. Osborne and M. A. Nielsen, Phys. Rev. A **66**, 032110 (2002).
[10] V. Vedral, New J. Phys. **6**, 102 (2004).
[11] X. Wang and P. Zanardi, Phys. Lett. A **301**, 1 (2002).
[12] X. Wang, Phys. Rev. A **66**, 034302 (2002).
[13] V. Vedral, New J. Phys. **6**, 22 (2004).
[14] Č. Brukner and V. Vedral, e-print quant-ph/0406040.
[15] S. Ghosh *et al.*, Nature (London) **425**, 48 (2003).
[16] M. Horodecki, P. Horodecki, and R. Horodecki, Phys. Lett. A **223**, 1 (1996).
[17] G. Xu *et al.*, Phys. Rev. Lett. **84**, 4465 (2000).
[18] W. K. Wootters, Phys. Rev. Lett. **80**, 2245 (1998).
[19] L. Berger, S. A. Friedberg, and J. T. Schriemf, Phys. Rev. **132**, 1057 (1963).
[20] J. C. Bonner *et al.*, Phys. Rev. B **27**, 248 (1983).
[21] T. Barnes, J. Riera, and D. A. Tennant, Phys. Rev. B **59**, 11384 (1999).
[22] D. A. Tennant *et al.*, Phys. Rev. B **67**, 054414 (2003).
[23] P. J. Brown, in *Internation Tables for Crystallography*, edited by A. J. Wilson and E. Prince (Kluwer Academic Publishers, Boston, 1999), Vol. C.
[24] S. W. Lovesey, *Theory of Neutron Scattering from Condensed Matter* (Clarendon, Oxford, 1984).
[25] P. C. Hohenberg and W. F. Brinkman, Phys. Rev. B **10**, 128 (1974).
[26] For an application, see S. M. Girvin, A. H. MacDonald, and P. M. Platzman, Phys. Rev. B **33**, 2481 (1986).
[27] A. B. Harris, Phys. Rev. B **7**, 3166 (1973).
[28] J. F. Clauser *et al.*, Phys. Rev. Lett. **23**, 880 (1969).